

# Neurocoder: Learning General-Purpose Computation Using Stored Neural Programs

Hung Le and Svetha Venkatesh  
Applied AI Institute, Deakin University, Geelong, Australia  
{thai.le,svetha.venkatesh}@deakin.edu.au

## Abstract

Artificial Neural Networks are uniquely adroit at machine learning by processing data through a network of artificial neurons. The inter-neuronal connection weights represent the learnt Neural Program that instructs the network on how to compute the data. However, without an external memory to store Neural Programs, they are restricted to only one, overwriting learnt programs when trained on new data. This is functionally equivalent to a special-purpose computer. Here we design Neurocoder, an entirely new class of general-purpose conditional computational machines in which the neural network “codes” itself in a data-responsive way by composing relevant programs from a set of shareable, modular programs. This can be considered analogous to building Lego structures from simple Lego bricks. Notably, our bricks change their shape through learning. External memory is used to create, store and retrieve modular programs. Like today’s stored-program computers, Neurocoder can now access diverse programs to process different data. Unlike manually crafted computer programs, Neurocoder creates programs through training. Integrating Neurocoder into current neural architectures, we demonstrate new capacity to learn modular programs, handle severe pattern shifts and remember old programs as new ones are learnt, and show substantial performance improvement in solving object recognition, playing video games and continual learning tasks. Such integration with Neurocoder increases the computation capability of any current neural network and endows it with entirely new capacity to reuse simple programs to build complex ones. For the first time a Neural Program is treated as a datum in memory, paving the ways for modular, recursive and procedural neural programming.

## 1 Introduction

From its inception in 1943 until recently, the fundamental architectures of Artificial Neural Networks remained largely unchanged - a program is executed by passing data through a network of artificial neurons whose inter-neuronal connection weights are learnt through training with data. These inter-neuronal connection weights, or Neural Programs, correspond to a program in modern computers [30]. Memory Augmented Neural Networks (MANN) are an innovative solution allowing networks to access external memory for manipulating data [10, 11]. But they were still unable to store Neural Programs in such external memory, and this severely limits machine learning. Storing inter-neuronal connection weights only in their network does not permit modular separation of Neural programs and is analogous to a computer with one fixed program. Recent works introduce *conditional computation*, adjusting or activating parts of a network in an input-dependent manner [35, 31, 3, 12], but networks remain

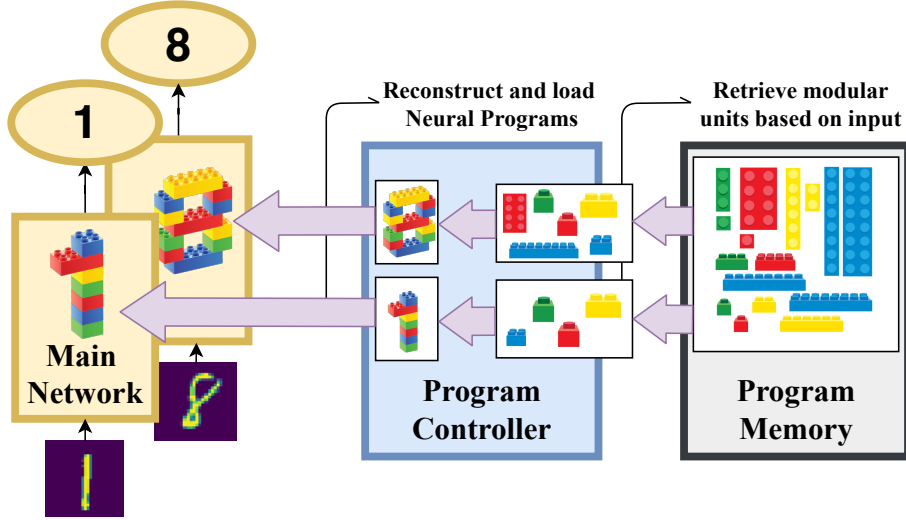


Figure 1: Overview structure of Neurocoder. Main Network processes inputs to produce outputs. Program Memory stores modular units. Program Controller reads modular units from the Program Memory, composing Neural Programs for the Main Network in a data-driven manner. Each Neural Program is designed for specific input. Intuitively, it is analogous to building Lego structures corresponding to inputs from basic Lego bricks.

monolithic. Current networks forget when retrained, old inter-neuronal connection weights are merged with new ones or erased.

The brain is modular, not a monolithic system [7, 5]. Neuroscience research indicates that the brain is divided into functional modules [18, 6, 8]. If the neural program for each module is kept in separate networks, networks proliferate. Modular neural networks combine the output of multiple expert networks, but as the experts grow, the networks grow drastically [19, 13, 32, 27]. This requires huge computational storage and introduces redundancy as these experts do not share common basic programs.

*A pathway out of this bind is to keep such basic programs in memory and combine them as required.* This brings neural networks towards modern general-purpose computers that use the stored-program principle [33, 36] to efficiently access reusable programs in external memory. Here we show how Neurocoder, a new neural framework, introduces an entirely new class of general-purpose conditional computation machines in which an entire main neural network can be “coded” in an input-dependent manner. Efficient decomposition of Neural Programs creates shareable modular components that can reconstruct the whole program space. These components change their “shapes” based on training and are stored in an external Program Memory. Then, in a data-responsive way, a Program Controller retrieves relevant modular components to reconstruct the Neural Program. The process is analogous to shape-shifting Lego bricks that can be reused to build unlimited shapes and structures (See Fig. 1).

Using modular components vastly increases the learning capacity of the neural network by allowing re-utilisation of parameters, effectively curbing network growth as programs increase. The construction of modular components and the input-specific reconstruction of Neural Programs from the components is learnt through training via traditional backpropagation [28] as the architecture is end-to-end

differentiable.

## 2 System

A Neurocoder is a neural network (Main Network) coupled to an external Program Memory through a Program Controller. The *working program* of the Main Network processes the input data to produce the output. This working program is “coded” by the Program Controller by creating an input-dependent *active program* from the Program Memory (Fig. 2).

### Neurocoder stores Singular Value Decomposition of Neural Programs in Program Memory

The Neural Program needs to be stored efficiently in Program Memory. This is challenging as there may be millions of inter-neuronal connection weights, thus storing them directly ([23]) is grossly inefficient. Instead, the Neurocoder forms the basis of a subspace spanned by Neural Programs and stores the singular values and vectors of this subspace in memory slots of the Program Memory (hereafter referred to as *singular programs*). Based on the input, relevant singular programs are retrieved, a new program is reconstructed and then loaded in the Main Network to process the input. This representational choice significantly reduces the number of stored elements and allows each singular program to effectively represent a unitary function of the active program.

The *active program* matrix  $\mathbf{P}$  can be composed by standard low-rank approximation as

$$\mathbf{P} = \mathbf{U}\mathbf{S}\mathbf{V}^T \quad (1)$$

where  $\mathbf{U}$  and  $\mathbf{V}$  are matrices of the left and right singular vectors, and  $\mathbf{S}$  the matrix of singular values. The Program Memory is crafted as three *singular program memories*  $\{\mathbf{M}_U, \mathbf{M}_V, \mathbf{M}_S\}$  to store and retrieve these components. *The process “codes” the active program using singular programs from  $\{\mathbf{M}_U, \mathbf{M}_V, \mathbf{M}_S\}$ .*

The Program Memory also maintains the status for each singular program in terms of access and usage. To access a singular program, *program keys* ( $k$ ) are used. These keys are low-dimensional vectors that represent the singular program function and computed by a neural network that effectively compresses the content of memory slots. The *program usage* ( $m$ ) measures memory utilisation, recording how much a memory slot is used in constructing a program. The components of the Program Memory are summarised in Fig. 2 (c).

### Recurrent multi-head program attention mechanisms for program storage and retrieval

Neural networks use the concept of *differentiable attention* to access memory [10, 1, 24]. This defines a weighting distribution over the memory slots essentially weighting the degree to which each memory slot participates in a read or write operation. This is unlike conventional computers that use a unique address to access a single memory slot.

Here we use two kinds of attention. First is *content-based attention* [10, 11] to ensure that the singular program is selected based on its functionality and the data input. This is achieved by producing a query vector based on the input and comparing it to the program keys ( $k$ ) using cosine similarity. Higher cosine similarity scores indicate higher attention weights to the singular programs associated with those program keys. Second, to encourage better memory utilisation, higher attention weights are assigned to slots with lower program usage ( $m$ ) through *usage-based attention* [11, 29]. The attention

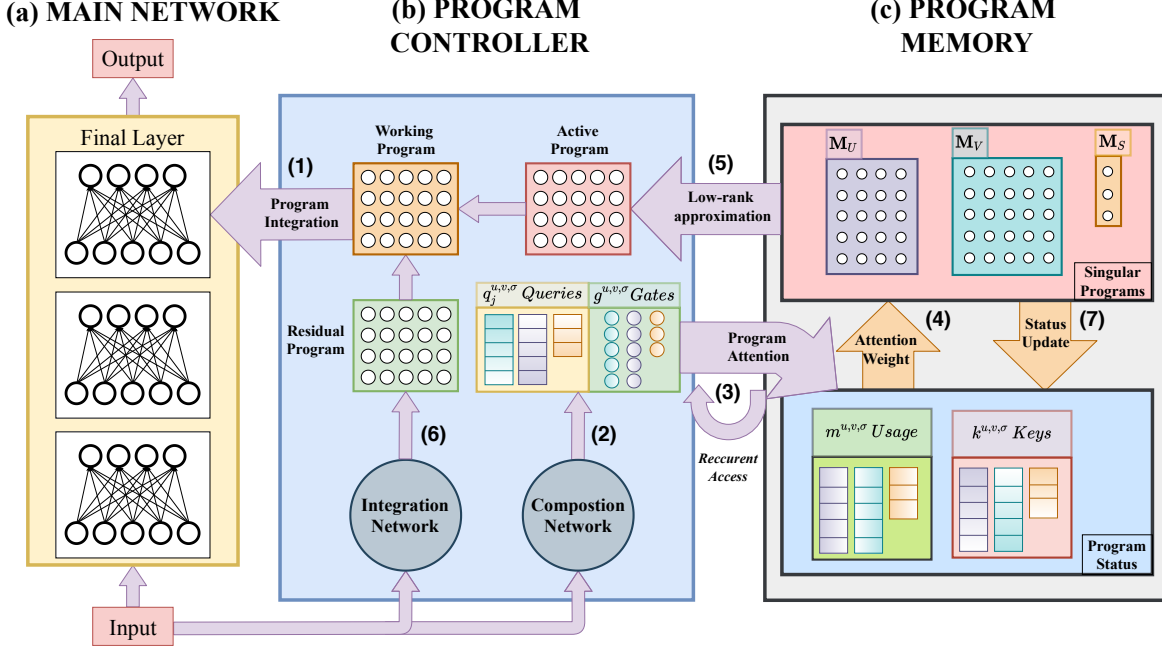


Figure 2: Neurocoder (a) The *Main Network* uses a *working program* to compute the output for the input. Here only the final layer of the Main Network is adaptively loaded with the working program (1). Other layers use traditional Neural Programs as connection weights (fixed-after-training). (b) The Program Controller’s *composition network* controls access to the Program Memory, emitting queries and interpolating gate control signals in response to the input (2). It then performs recurrent multi-head program attention to the Program Status (3), triggering attention weights to the Singular Programs (4). The attended Singular Programs form an *active program* using low-rank approximation (5). This active program is then used to derive the *working program* from a *residual program* produced by the Program Controller’s *integration network* (6). (c) The Program Memory stores the representations (singular programs) required to reconstruct the active program to be used by the Program Controller. Access is controlled through the Program Status including keys ( $k$ ), and slot usage ( $m$ ) that are updated during the training and computation (7).

weights from the two schemas are then combined using interpolating gates to compose the final attention weights to the Program Memory.

We adapt multi-head attention [10, 34] that applies multiple attentions in parallel to retrieve  $H$  singular components. Besides, we introduce a recurrent attention mechanism, in which multi-head access is performed recurrently in  $J$  steps. The  $j$ -th set of  $H$  retrieved components is conditioned on the previous ones. This recurrent, multi-head attention allows the composition network to attend to multiple memory slots recurrently, incrementally searching for optimal components for building relevant active programs.

### Neurocoder learns to “code” a relevant working program via training

The structure of the Program Memory and the role of the Program Controller facilitates the automatic construction of working programs via training. The Program Controller controls memory access through its *composition network* that creates the *attention weight* defining how to weight the singular programs. Applying the recurrent multi-head attention described earlier, multiple singular programs are retrieved to construct an active program (Eq. 1). Then the Program Controller generates a *residual program* using its *integration network* to transform the active program into the working program of the Main Network. This transformation enables creation of flexible higher-rank working programs, which compensates for the low-rank coding process. The structure of the Program Controller is illustrated in Fig. 2 (b).

The singular programs are trained to represent unitary functions necessary for any computation whilst the composition and integration networks are trained to compose the relevant programs from the singular programs to compute the current input. The parameters of the networks, and the stored singular programs are adjusted during end-to-end training. Initially, all the parameters will be random, leading to creation of representations and working programs that produce huge training loss. However, as training proceeds, these parameters get adjusted and the network gets trained. Training is traditional and minimises the total loss using gradient descent as

$$\mathcal{L} = \mathcal{L}_{task} + a\mathcal{L}_o \quad (2)$$

where  $\mathcal{L}_{task}$  represents the supervised training loss and  $\mathcal{L}_o$  represents a term weighted by a hyper-parameter  $a$  to enforce orthogonality of the singular vectors.

### Neurocoder can be integrated with any neural network

The Main Network of the Neurocoder can be any current neural network. One or more layers of the neural network can be replaced in this way and re-coded with working programs from the Neurocoder in a data-responsive way (Fig. 2 (a)). Here we show how Neurocoders re-code programs for single or all layers of diverse networks like Multi-layer Perceptron, Convolutional Neural Networks and Reinforcement Learning architectures. It is significant that this can be done by plugging Neurocoder into current architectures without modification of training paradigms or major addition to the number of parameters. *Thus any state-of-the-art neural architecture plus Neurocoder can re-code itself from a suite of programs.*

### 3 Methods

#### Program Coding as Low-rank Approximation

The Program Memory stores singular programs in three singular program memories  $\{\mathbf{M}_U, \mathbf{M}_V, \mathbf{M}_S\}$ . At some time  $t$ , we compose the active program  $\mathbf{P}_t$  by low-rank approximation as follows,

$$\mathbf{P}_t = \mathbf{U}\mathbf{S}\mathbf{V}^T \quad (3)$$

$$= \sum_n^{r_m} \sigma_{tn} u_{tn} v_{tn}^\top \quad (4)$$

where  $r_m$  is the total number of components we want to retrieve,  $\{\sigma_{tn}\}_{n=1}^{r_m}$  the singular values,  $\{u_{tn}\}_{n=1}^{r_m}$  and  $\{v_{tn}\}_{n=1}^{r_m}$  the singular vectors of  $\mathbf{S}$ ,  $\mathbf{U}$ , and  $\mathbf{V}$ , respectively.

By limiting  $r_m$ , we put a constrain on the rank of the active program. To enforce orthogonality of the singular vectors, we minimise the orthogonal loss

$$\mathcal{L}_o = \mathbf{M}_U \mathbf{M}_U^\top - \mathbf{I} + \mathbf{M}_V \mathbf{M}_V^\top - \mathbf{I} \quad (5)$$

Since the active program is dynamically composed at time  $t$  for the computation of input  $x_t$ , it resembles fast-weights in neural networks [35]. Unlike fast-weights, the working program consists of singular programs stored in Program Memory representing the stored-program principle [33, 36]. It differs from an earlier attempt to implement a memory for programs, the Neural Stored-program Memory [23] which stores each item as a working program itself. It extends the concept of slot-based neural memory [10, 11, 21, 22] to storing neural programs as data.

We now use attention weights ( $w_{tin}^u$ ,  $w_{tin}^v$ ,  $w_{tin}^\sigma$  jointly denoted as  $w_{tin}^{u,v,\sigma}$ ) to each slot of the singular program memories  $\mathbf{M}_U$ ,  $\mathbf{M}_V$  and  $\mathbf{M}_S$  to read each singular vector as

$$u_{tn} = \sum_{i=1}^{P_u} w_{tin}^u \mathbf{M}_U(i) \quad (6)$$

$$v_{tn} = \sum_{i=1}^{P_v} w_{tin}^v \mathbf{M}_V(i) \quad (7)$$

For the singular values, we enforce  $\sigma_{t1} > \sigma_{t2} > \dots > \sigma_{tr_m} > 0$  by using

$$\sigma_{tn} = \begin{cases} \text{softplus} \left( \sum_{i=1}^{P_s} w_{tin}^\sigma \mathbf{M}_S(i) \right) & n = r_m \\ \sigma_{tn+1} + \text{softplus} \left( \sum_{i=1}^{P_s} w_{tin}^\sigma \mathbf{M}_S(i) \right) & n < r_m \end{cases} \quad (8)$$

Here,  $P_u$ ,  $P_v$  and  $P_s$  are the number of memory slots of  $\mathbf{M}_U$ ,  $\mathbf{M}_V$  and  $\mathbf{M}_S$ , respectively. For simplicity, in this paper, we set  $P = P_u = P_v = P_s$  as the number of memory slots of the Program Memory. The attention weights  $w_{tin}^{u,v,\sigma}$ , shorten form for  $w_{tijh}^{u,v,\sigma}$ , are determined by program memory attention mechanisms, which will be discussed in the upcoming sections.

#### Recurrent Access to the Program Memory via the composition network

To perform program attention, the Program Controller employs a composition network (denoted as  $f_{\theta^{u,v,\sigma}}$ ), which takes the current input  $x_t$  and produce *program composition control signals* ( $\xi_t^p$ ). If

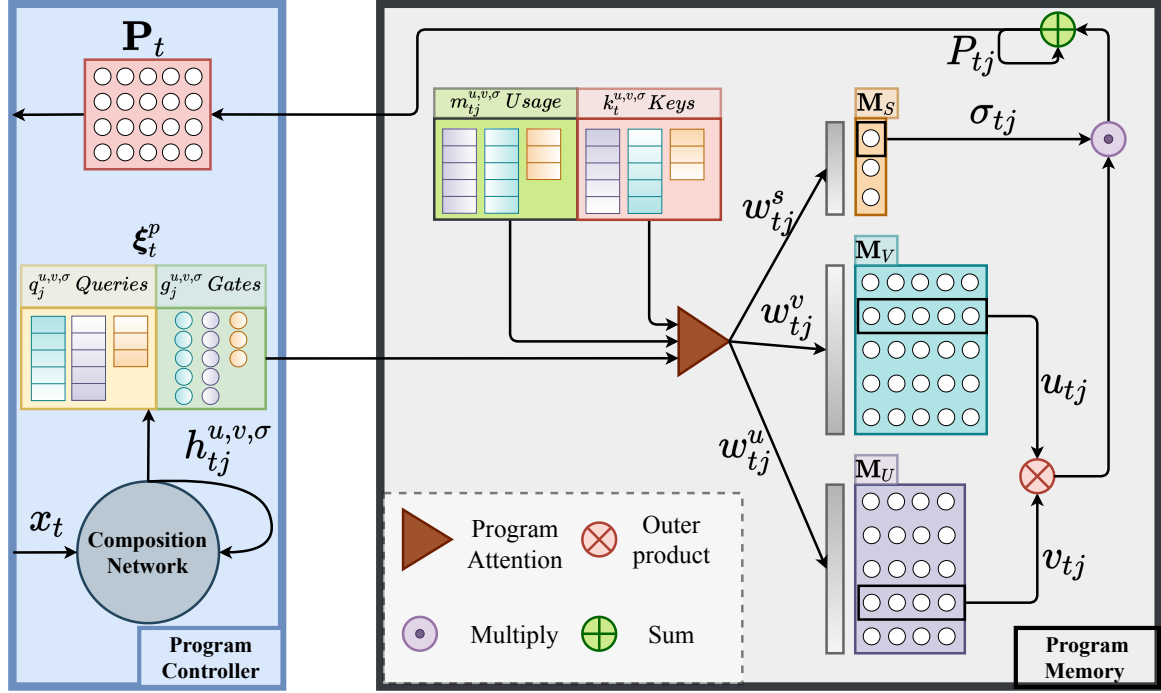


Figure 3: Active program coding. The Program Controller uses the composition network (a recurrent neural network) to process the input  $x_t$  and generate composition signal  $\xi_t^p$ , which is composed of the queries ( $q$ ) and the interpolating gates ( $g$ ). The similarity of the query to program memory keys ( $k$ ) is then computed together with the memory usage ( $m$ ) from which attention weights for the Program Memory are derived. The active program  $P_t$  is then “coded” through low-rank approximation using the  $j$ -th component accessed by recurrent attentions. For simplicity, one attention head is shown ( $H = 1$ ).

$f_{\theta^{u,v,\sigma}}$  performs all attentions concurrently via multi-head attention (as in [10, 34]), it may lead to program collapse [23]. To have a better control of the component formation and alleviate program collapse, we propose to recurrently attend to the program memory. To this end, we implement  $f_{\theta^{u,v,\sigma}}$  as a recurrent neural network (LSTM [15]) and let it access the program memory  $J$  times, resulting in  $\xi_t^p = \{\xi_{tj}^p\}_{j=1}^J$ . At access step  $j$ , the recurrent network updates its hidden states and generates  $\xi_{tj}^p$  using recurrent dynamics as

$$\xi_{tj}^p, h_j^{u,v,\sigma} = f_{\theta^{u,v,\sigma}}(x_t, h_{j-1}^{u,v,\sigma}) \quad (9)$$

where  $h_0^{u,v,\sigma}$  is initialized as zeros and  $\xi_{tj}^p$  is the program composition control signal at step  $j$  that depends on both on the input data  $x_t$  and the the previous state  $h_{j-1}^{u,v,\sigma}$ . Particularly, the control signal contains the queries and the interpolation gates used to compute the program attention ( $w_{tin}^{u,v,\sigma}$ ):  $\xi_{tj}^p = \{q_{tjh}^{u,v,\sigma}, g_{tjh}^{u,v,\sigma}\}_{h=1}^H$ . Here, at each attention step, we perform multi-head attention with  $H$  as the number of attention heads or retrieved components and thus, each  $\xi_{tj}^p$  consists of  $H$  pairs of queries and gates. Hence, the total number of retrieved components  $r_m = J \times H$ .

### Attending to Programs by “Name”

Inspired by the content-based attention mechanism for data memory [10], we use the query to look for the singular programs. In computer programming, to find the appropriate program for some computation, we often refer to the program description or at least the name of the program. Here, we create the “name” for our neural programs by compressing the program content to a low-dimensional key vector. As such, we employ a neural network ( $f_\varphi$ ) to compute the program memory keys as

$$k_i^{u,v,\sigma} = f_{\varphi^{u,v,\sigma}}(\mathbf{M}_{U,V,S}(i)) \quad (10)$$

where  $k_i^{u,v,\sigma} = \left\{ \{k_i^u \in \mathbb{R}^K\}_{i=1}^{P_u}, \{k_i^v \in \mathbb{R}^K\}_{i=1}^{P_v}, \{k_i^\sigma \in \mathbb{R}^K\}_{i=1}^{P_\sigma} \right\}$ . Here,  $f_{\varphi^{u,v,\sigma}}$  learns to compress each memory slot of the singular program memories into a  $K$ -dimensional vector. As the singular programs evolve, their keys get updated. In this paper, we calculate the program keys after each learning iteration during training.

Finally the content-based program memory attention  $c_{tjh}^{u,v,\sigma} = \{c_{tjh}^u, c_{tjh}^v, c_{tjh}^\sigma\}$  is computed using cosine distance between the program keys  $k_i^{u,v,\sigma}$  and the queries  $q_{tjh}^{u,v,\sigma}$  as

$$c_{tjh}^{u,v,\sigma} = \text{softmax}^{(i)} \left( \frac{q_{tjh}^{u,v,\sigma} \cdot k_i^{u,v,\sigma}}{\|q_{tjh}^{u,v,\sigma}\| \cdot \|k_i^{u,v,\sigma}\|} \right) \quad (11)$$

### Making Every Program Count

Similarly to [11, 29], in addition to the content-based attention, we employ a least-used reading strategy to encourage the Program Controller to assign different singular programs to different components. In particular, we calculate the memory usage for each program slot across attentions as

$$m_{tjh}^{u,v,\sigma} = \max_{\tilde{j} \leq j} \left( w_{tj\tilde{j}h}^{u,v,\sigma} \right) \quad (12)$$



where  $m^{u,v,\sigma} = \{m^u \in \mathbb{R}^{P_u \times 1}, m^v \in \mathbb{R}^{P_v \times 1}, m^\sigma \in \mathbb{R}^{P_\sigma \times 1}\}$ . Since we want to consider only  $l_I$  amongst  $P$  memory slots that have smallest usages, let  $\hat{m}_{tjh}^{u,v,\sigma(l_I)}$  denote the value of the  $l_I$ -th smallest usage, then the least-used attention is computed as

$$l_{tjh}^{u,v,\sigma} = \begin{cases} \max_i \left( m_{tjh}^{u,v,\sigma} \right) - m_{tjh}^{u,v,\sigma} & ; m_{tjh}^{u,v,\sigma} \leq \hat{m}_{tjh}^{u,v,\sigma(l_I)} \\ 0 & ; m_{tjh}^{u,v,\sigma} > \hat{m}_{tjh}^{u,v,\sigma(l_I)} \end{cases} \quad (13)$$

The final program memory attention is computed as

$$w_{tjh}^{u,v,\sigma} = \text{sigmoid} \left( g_{tjh}^{u,v,\sigma} \right) c_{tjh}^{u,v,\sigma} + \left( 1 - \text{sigmoid} \left( g_{tjh}^{u,v,\sigma} \right) \right) l_{tjh}^{u,v,\sigma} \quad (14)$$

Since the usage record are computed along the memory accesses, the multi-step Neurocoder utilises this attention mechanism better than the single-step Neurocoder, leading to different attention behaviors (see Sec. 4). The whole process of composing the active program  $\mathbf{P}_t$  is illustrated in Fig. 3.

### Program Integration via the integration network

Since the working program  $\mathbf{P}_t$  only contains top  $r_m$  principal components, it may be not flexible enough for sophisticated computation. We propose to enhance  $\mathbf{P}_t$  with a residual program  $\mathbf{R}$ — a traditional connection weight trained as the integration network’s parameters. The residual program represents the sum of the remaining less important components. To this end, we suppress  $\mathbf{R}$  with a multiplier that is smaller than  $\sigma_{tr_m}$ — the smallest singular value of the main components - resulting in the integration formula

$$W_t = \mathbf{P}_t + w_t^r \sigma_{tr_m} \mathbf{R} \quad (15)$$

where  $w_t^r = \text{sigmoid} (f_\phi(x_t))$  is an adaptive gating value that controls the contribution of the residual program.  $f_\phi$  is the integration network in the Program Controller and hence, in our implementation, the integration control signal sent by the Program Controller is  $\boldsymbol{\lambda}_t^p = \{w_t^r, \sigma_{tr_m}\}$ . We note that in our experiments, the program integration is sometimes disabled ( $W_t$  is directly set to  $\mathbf{P}_t$ ) to eliminate the effect of  $\mathbf{R}$  or reduce the number of parameters.

The working program  $W_t$  is then used by the Main Network to execute the input data  $x_t$ . For example, with linear classifier Main Network, the execution is  $y_t = x_t W_t$ . Table 1 summarises the notations used for important parameters of Neurocoder.

The Main Network can be any neural network in which one or more layers of this network can be replaced by the Neurocoder. In our experiments, we always apply Neurocoder to all layers of multi-layer perceptrons (MLP) or just the final output layer of CNNs (LeNet, DenseNet, ResNet), RNNs (GRU), and the policy/value networks of A3C. Other competitors such as MOE, NSM and HyperNet are applied to the Main Networks in the same manner.

## 4 Results

To demonstrate the flexibility of this framework, we consider different learning paradigms: instance-based, sequential and continual learning. We do not focus on breaking performance records by augmenting state-of-the-art models with Neurocoder. Rather our inquiry is on re-coding layers of diverse neural networks with the Neurocoder’s programs and testing on varied data types to demonstrate its intrinsic properties (details of the following section are in Appendix).

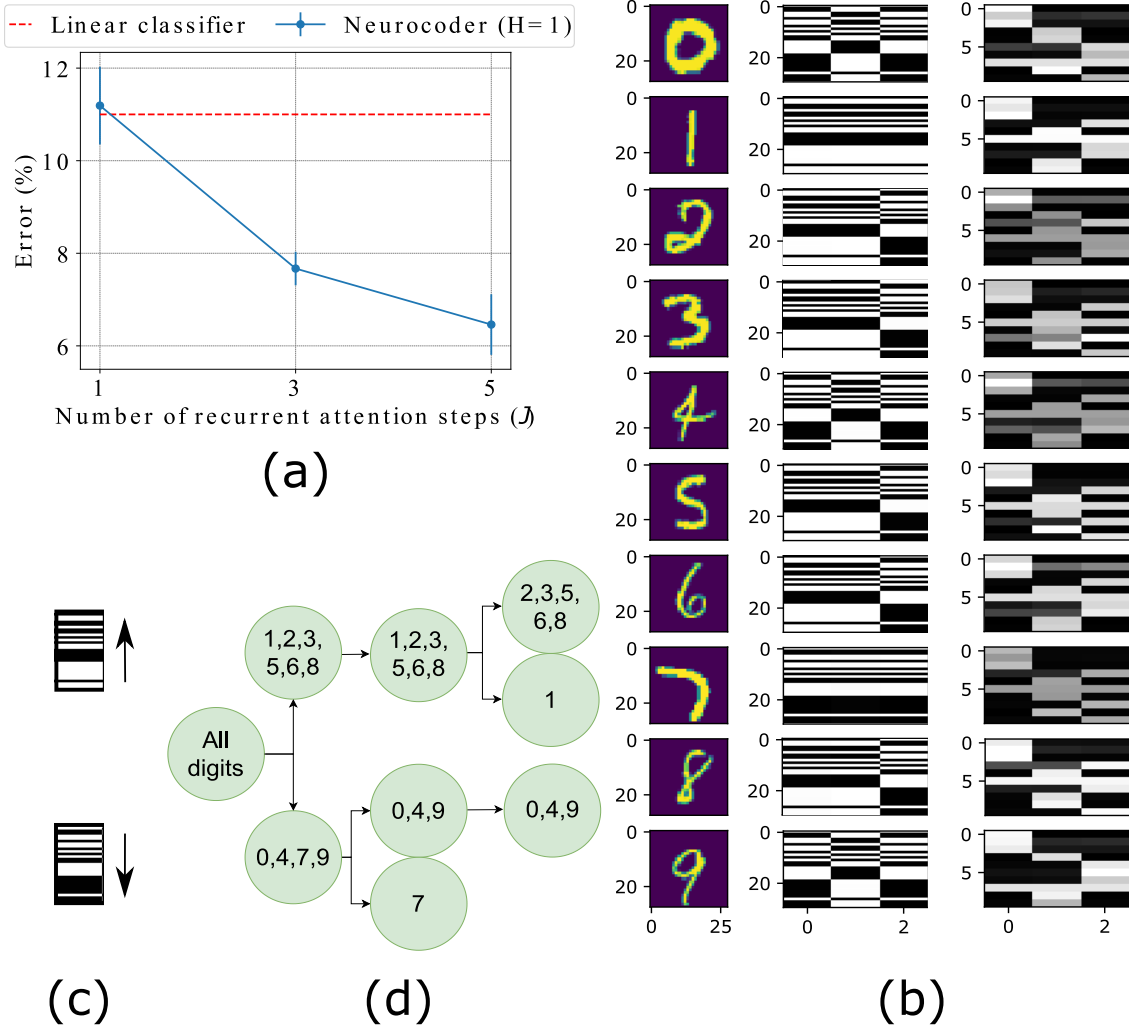


Figure 4: (a) MNIST test set classification error *vs* the number of steps ( $J$ ) in Neurocoder (blue), compared with a linear classifier (red). (b) *1st column*: Digit images; *Middle column*: Single-step attention weights for 30 slots in  $\mathbf{M}_U$  (vertical axis) for first 3 singular vectors (horizontal axis) for each digit; *Last column*: Multi-step attention weights for 10 slots in  $\mathbf{M}_U$  (vertical axis) for first 3 singular vectors (horizontal axis). Multi-step attention is able to produce far more diverse patterns with fewer slots - 10 slots compared to single-step 30 slots. (c) Two attention patterns of single-step Neurocoder. (d) The binary decision tree derived from single-step Neurocoder's attention patterns. The two patterns across components represent the decisions going up and down across the binary tree.

## 4.1 Instance-based learning - Object Recognition

We tested Neurocoder on instance-based learning through classical image classification tasks using MNIST [25] and CIFAR [20] datasets. The first experiment interpreted Neurocoder’s behaviour in classifying digits into 10 classes (0 – 9) using linear classifier Main Network. With equivalent model size, Neurocoder using the novel recurrent attention surpasses the performance of the linear classifier [25] by up to 5% (Fig. 4 (a)).

To differentiate the input, Neurocoder attends to different components of the active program to guide the decision-making process. Fig. 4 (b) shows single-step and multi-step attention to the first 3 singular vectors for each digit across memory slots. Multi-step attention produces richer patterns compared to single-step Neurocoder that manages only 2 attention weight patterns (Fig. 4 (c)).

Fig. 4 (d) illustrates how Neurocoder performs modular learning by showing the attention assignment for top 3 singular vectors as a binary decision tree. Digits under the same parental node share similar attention paths, and thereby similar active programs. Some digits look unique (e.g. 7) resulting in active programs composed of unique attention paths, discriminating themselves early in the decision tree. Some digits (e.g. 0 and 9) share the same attention pattern for the first 3 components and are thus unclassifiable in the binary tree. They can only be distinguished by considering more singular vectors.

We integrated Neurocoder with deep networks - 5-layer *LeNet* and 100-layer *DenseNet* - and tested on complex CIFAR datasets. Neurocoder significantly outperformed the original Main Networks with performance gain around 2 – 5%. Compared with recent conditional computing models such as Mixture of Experts (MOE [32]) and Neural Stored-program Memory (NSM [23]), Neurocoder required a tenth of the number of parameters and performed better by up to 7% (see Table 2).

## 4.2 Sequential learning - Adaption to sequence changes and game playing using reinforcement learning

Recurrent neural networks (RNN) can learn from sequential data by updating the hidden states of the networks. However, this does not suffice when local patterns shift, as is often the case. We now demonstrate that Neurocoder helps RNNs overcome this limitation by composing diverse programs to handle sequence changes.

**Synthetic polynomial auto-regression** We created a simple auto-regression task in which data points are sampled from polynomial function chunks that change over time. The Main Network is a strong *RNN-Gated Recurrent Unit* (*GRU* [4]). We found that GRU integrated with a single-step or multi-step Neurocoder learned much faster than its original version and HyperNet counterparts [12] (Fig. 6).

Visualising the first singular vector attention weights in  $\mathbf{M}_U$ , we find that the multi-step attention Neurocoder changes its attention following polynomial changes - it attends to the same singular program when processing data from the same polynomial and alters attention for data from a different polynomial (Fig. 5(a)). In contrast, the single-step Neurocoder only changes its attention when there is a remarkable change in  $y$ -coordinate values (Fig. 5(b)). We hypothesise that when recurrence is employed, usage-based attention takes effect, stipulating better memory utilisation and diverse attentions over timesteps. Although single-step Neurocoder converges well, it did not discover the underlying structure of the data, and thus underperformed the multi-step Neurocoder.

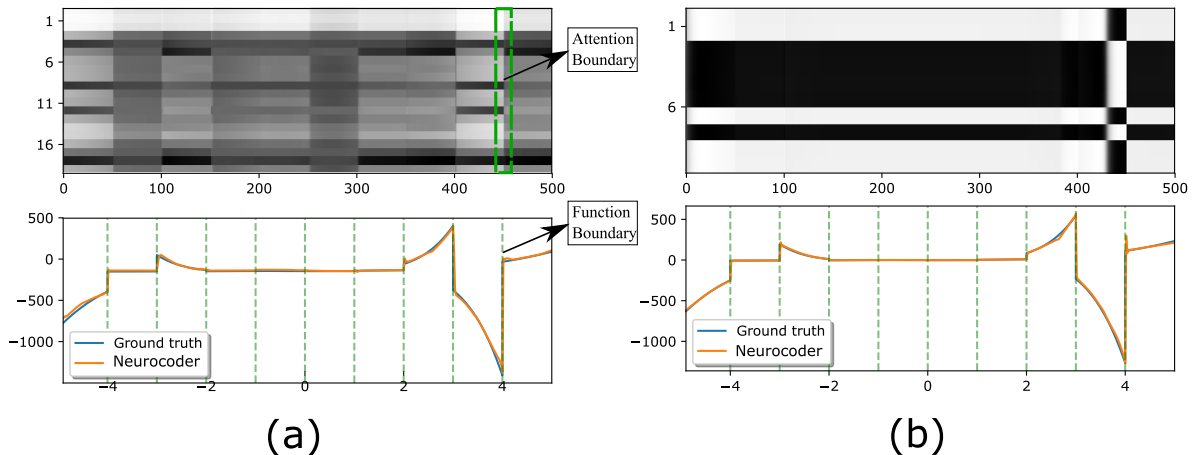


Figure 5: Visualisation for (a) multi-step ( $J = 5$ , 20 memory slots) and (b) single-step ( $J = 1$ , 10 memory slots) cases showing while processing a sequence of the polynomial auto-regression task. The Neurocoder’s attentions to  $\mathbf{M}_U$  that form the first component of the active program are shown over sequence timesteps (*upper*) with Neurocoder’s  $y_t$  prediction (orange) and ground truth (blue) (*lower*). The vertical dash green lines separate polynomial chunks. Each chunk represents a local pattern, and thus ideally requires a specific active program to compute the input  $x_t$ . Although both predict well, only the multi-step Neurocoder discovers the chunk boundaries, assigning program attention to the first component in accordance with sequence changes.

**Atari game reinforcement learning** We used reinforcement learning as a further testbed to show the ability to adapt to environmental changes. We performed experiments on several Atari 2600 games [2] wherein the agent (or Main Network) was implemented as the *Asynchronous Advantage Actor-Critic* (A3C [26]). In the Atari platform, agents are allowed to observe the screen snapshot of the games and act to earn the highest score. We augmented the A3C by employing Neurocoder’s working programs for the actor and critic networks, aiming to decompose the policy and value function into singular programs that were selected depending on the game state.

*Frostbite and Montezuma’s Revenge.* These games are known to be challenging for A3C and other algorithms [26]. We trained A3C and HyperNet-based A3C for over 300 million steps, yet these models did not show any sign of learning, performing equivalently to random agents. For such complicated environments with sparse rewards, both the monolithic neural networks and the unstored fast-weights fail to learn (almost zero scores). In contrast, Neurocoder enabled A3C to achieve from 1,500 to 3,000 scores on these environments (Fig. 7), confirming the importance of decomposing a complex solution to smaller, simple stored programs.

### 4.3 Continual learning

In continual learning, standard neural networks often suffer from “catastrophic forgetting” in which they cannot retain knowledge acquired from old tasks upon learning new ones [9]. Our Neurocoder offers natural mitigation of such catastrophic forgetting in neural networks by storing task-dependent singular programs in separated program memory slots.

**Split MNIST** We first considered the split MNIST dataset—a standard continual learning benchmark wherein the original MNIST was split into a 5 2-way classification tasks, consecutively presented to a *Multi-layer Perceptron* Main Network (MLP). We followed the benchmarking as in [16] in which various optimisers and state-of-the-art continual learning methods were examined under incremental task and domain scenarios. We measured the performance of the MLP versus Neurocoder and NSM under each continual learning method.

In both scenarios, Neurocoder was compatible with all continual learning methods, demonstrating superior performance over MLP and NSM with performance gain between 1 to 16% (see Table 3 and 4).

**Split CIFAR** We verified the scalability of Neurocoder to more challenging datasets. We split CIFAR datasets as in the split MNIST, wherein 5-task 2-way split CIFAR10 and a 20-task 5-way split CIFAR100 were created. We integrate Neurocoder with *ResNet* [14]—a very deep CNN architecture as the Main Network.

When we stressed the orthogonal loss ( $a = 10$ ) and used bigger program memory (100 slots), Neurocoder improved ResNet classification by 15% and 10% on CIFAR10 and CIFAR100, respectively. When we integrated Neurocoder with Synaptic Intelligence (SI [37]), the performance was further improved, maintaining a stable performance above 80% accuracy for CIFAR10 and outperforming using SI alone by 10% for CIFAR100 (see Fig. 8).

## 5 Discussion

Our experiments demonstrate that Neurocoder is capable of re-coding Neural Programs in distinctive neural networks, amplifying their capabilities in diverse learning scenarios: instance-based, sequential and continual learning. This consistently results in significant performance increase, and further creates novel robustness to pattern shift and catastrophic forgetting. This unprecedented ability for each architecture to re-code itself is made possible without changing the way it is trained, or majorly increasing the number of parameters it needs to learn.

The MNIST problem illustrates the reasoning process of Neurocoder when classifying digit images wherein its singular program assignment resembles a binary tree decision-making process - it shows how some singular programs are shared, others are not. The polynomial auto-regression problem highlights the importance of efficient memory utilisation in re-constructing the working program enabling discovery of hidden structures in sequential data. Training our framework with reinforcement learning, we enable neural agents to solve complex games wherein traditional methods fail or learn slowly. Finally, continual learning problems show that Neurocoder mitigates catastrophic forgetting efficiently under different learning settings/algorithms.

Our solution offers a single framework that is scalable and adaptable to various problems and learning paradigms. Unlike previous attempts to employ a bank of separate big programs [19, 32, 23], Neurocoder maintains only shareable, smaller components that can reconstruct the whole program space, thereby heavily utilising the parameters and preventing the model from proliferating. We can further extend Neurocoder’s ability by allowing a growing Program Memory, in which the model decides to add or erase memory slots as the number of data patterns grows or shrinks beyond the current program space’s capacity. Such a system represents a more flexible general-purpose computer that can dynamically allocate computing resources by itself without human pre-specification.

## References

- [1] Dzmitry Bahdanau, Kyunghyun Cho, and Yoshua Bengio. Neural machine translation by jointly learning to align and translate. In *International Conference on Learning Representations*, 2015.
- [2] Marc G Bellemare, Yavar Naddaf, Joel Veness, and Michael Bowling. The arcade learning environment: An evaluation platform for general agents. *Journal of Artificial Intelligence Research*, 47:253–279, 2013.
- [3] Yoshua Bengio, Nicholas Léonard, and Aaron Courville. Estimating or propagating gradients through stochastic neurons for conditional computation. *arXiv preprint arXiv:1308.3432*, 2013.
- [4] Kyunghyun Cho, Bart van Merriënboer, Caglar Gulcehre, Dzmitry Bahdanau, Fethi Bougares, Holger Schwenk, and Yoshua Bengio. Learning phrase representations using RNN encoder–decoder for statistical machine translation. In *Conference on Empirical Methods in Natural Language Processing (EMNLP)*, pages 1724–1734. Association for Computational Linguistics, October 2014.
- [5] JC Eccles. The modular operation of the cerebral neocortex considered as the material basis of mental events. *Neuroscience*, 6(10):1839–1855, 1981.
- [6] Gerald M Edelman. Neural darwinism: selection and reentrant signaling in higher brain function. *Neuron*, 10(2):115–125, 1993.
- [7] Gerald M Edelman and Vernon B Mountcastle. *The mindful brain: cortical organization and the group-selective theory of higher brain function*. Massachusetts Inst of Technology Pr, 1978.
- [8] Richard SJ Frackowiak. *Human brain function*. Elsevier, 2004.
- [9] Robert M French. Catastrophic forgetting in connectionist networks. *Trends in cognitive sciences*, 3(4):128–135, 1999.
- [10] Alex Graves, Greg Wayne, and Ivo Danihelka. Neural turing machines. *arXiv preprint arXiv:1410.5401*, 2014.
- [11] Alex Graves, Greg Wayne, Malcolm Reynolds, Tim Harley, Ivo Danihelka, Agnieszka Grabska-Barwińska, Sergio Gómez Colmenarejo, Edward Grefenstette, Tiago Ramalho, John Agapiou, et al. Hybrid computing using a neural network with dynamic external memory. *Nature*, 538(7626):471–476, 2016.
- [12] David Ha, Andrew M. Dai, and Quoc V. Le. Hypernetworks. In *International Conference on Learning Representations*, 2017.
- [13] Bart LM Happel and Jacob MJ Murre. Design and evolution of modular neural network architectures. *Neural networks*, 7(6-7):985–1004, 1994.
- [14] Kaiming He, Xiangyu Zhang, Shaoqing Ren, and Jian Sun. Deep residual learning for image recognition. In *Proceedings of the IEEE conference on computer vision and pattern recognition*, pages 770–778, 2016.
- [15] Sepp Hochreiter and Jürgen Schmidhuber. Long short-term memory. *Neural computation*, 9(8):1735–1780, 1997.

- [16] Yen-Chang Hsu, Yen-Cheng Liu, Anita Ramasamy, and Zsolt Kira. Re-evaluating continual learning scenarios: A categorization and case for strong baselines. In *NeurIPS Continual learning Workshop*, 2018.
- [17] Gao Huang, Zhuang Liu, Laurens Van Der Maaten, and Kilian Q Weinberger. Densely connected convolutional networks. In *Proceedings of the IEEE conference on computer vision and pattern recognition*, pages 4700–4708, 2017.
- [18] D.H. Hubel. *Eye, Brain, and Vision*. Scientific American Library series. Scientific American Library, 1988.
- [19] Robert A Jacobs, Michael I Jordan, Steven J Nowlan, and Geoffrey E Hinton. Adaptive mixtures of local experts. *Neural computation*, 3(1):79–87, 1991.
- [20] Alex Krizhevsky, Geoffrey Hinton, et al. Learning multiple layers of features from tiny images. 2009.
- [21] Hung Le, Truyen Tran, Thin Nguyen, and Svetha Venkatesh. Variational memory encoder-decoder. In *Advances in Neural Information Processing Systems*, pages 1508–1518, 2018.
- [22] Hung Le, Truyen Tran, and Svetha Venkatesh. Learning to remember more with less memorization. In *International Conference on Learning Representations*, 2018.
- [23] Hung Le, Truyen Tran, and Svetha Venkatesh. Neural stored-program memory. In *International Conference on Learning Representations*, 2020.
- [24] Hung Le, Truyen Tran, and Svetha Venkatesh. Self-attentive associative memory. In *Proceedings of Machine Learning and Systems 2020*, pages 2363–2372. 2020.
- [25] Yann LeCun, Léon Bottou, Yoshua Bengio, and Patrick Haffner. Gradient-based learning applied to document recognition. *Proceedings of the IEEE*, 86(11):2278–2324, 1998.
- [26] Volodymyr Mnih, Adria Puigdomenech Badia, Mehdi Mirza, Alex Graves, Timothy Lillicrap, Tim Harley, David Silver, and Koray Kavukcuoglu. Asynchronous methods for deep reinforcement learning. In *International conference on machine learning*, pages 1928–1937, 2016.
- [27] Clemens Rosenbaum, Tim Klinger, and Matthew Riemer. Routing networks: Adaptive selection of non-linear functions for multi-task learning. In *International Conference on Learning Representations*, 2018.
- [28] David E Rumelhart, Geoffrey E Hinton, and Ronald J Williams. Learning representations by back-propagating errors. *Nature*, 323(6088):533–536, 1986.
- [29] Adam Santoro, Sergey Bartunov, Matthew Botvinick, Daan Wierstra, and Timothy Lillicrap. Meta-learning with memory-augmented neural networks. In *International conference on machine learning*, pages 1842–1850, 2016.
- [30] Jiirgen Schmidhuber. Making the world differentiable: On using self-supervised fully recurrent neural networks for dynamic reinforcement learning and planning in non-stationary environments. 1990.

- [31] Jürgen Schmidhuber. Learning to control fast-weight memories: An alternative to dynamic recurrent networks. *Neural Computation*, 4(1):131–139, 1992.
- [32] Noam Shazeer, Azalia Mirhoseini, Krzysztof Maziarz, Andy Davis, Quoc V. Le, Geoffrey E. Hinton, and Jeff Dean. Outrageously large neural networks: The sparsely-gated mixture-of-experts layer. In *International Conference on Learning Representations*, 2017.
- [33] A.M Turing. On computable numbers, with an application to the entscheidungsproblem. In *Proceedings of the London Mathematical Society*, 1936.
- [34] Ashish Vaswani, Noam Shazeer, Niki Parmar, Jakob Uszkoreit, Llion Jones, Aidan N Gomez, Lukasz Kaiser, and Illia Polosukhin. Attention is all you need. In *Advances in neural information processing systems*, pages 5998–6008, 2017.
- [35] Christoph von der Malsburg. The correlation theory of brain function, 1981.
- [36] John Von Neumann. First draft of a report on the edvac. *IEEE Annals of the History of Computing*, 15(4):27–75, 1993.
- [37] Friedemann Zenke, Ben Poole, and Surya Ganguli. Continual learning through synaptic intelligence. *Proceedings of machine learning research*, 70:3987, 2017.



# Appendix

## Instance-based learning experiments

**Image classification-linear Main Network** We used the standard training and testing set of MNIST dataset. To train the models, we used the standard SGD with a batch size of 32. Each MNIST image was flattened to a 768-dimensional vector, which requires a linear classifier of 7,680 parameters to categorise the inputs into 10 classes. For Neurocoder, we used Program Memory with  $P = 6$  and  $K = 2$ . The Program Controller’s composition network was an LSTM with a hidden size of 8. We controlled the number of parameters of Neurocoder, which included parameters for the Program Memory and the Program Controller by reducing the input dimension using random projection  $z_t = x_t U$  with  $U \in \mathbb{R}^{768 \times 200}$  initialised randomly and fixed during the training. We also excluded the program integration to eliminate the effect of the residual program  $\mathbf{R}$ . Given the flattened image input  $x_t$ , Neurocoder generated the active program  $\mathbf{P}_t$ , predicting the class of the input as  $y_t = \text{argmax}(x_t \mathbf{P}_t)$ . The performance of the linear classifier was imported from [25] and confirmed by our own implementation.

**Image classification-deep Main Network** We used the standard training and testing sets of CIFAR datasets. We use Adam optimiser with a batch size of 128. *The deep Main Networks were adopted from the original papers, resulting in 3-layer MLP, 5-layer LeNet [25] and 100-layer DenseNet [17].* The other baselines for this task included a recent Mixture of Experts (MOE [32]) and the Neural Stored-program Memory (NSM [23]). For this case, we employed the program integration with the residual program  $\mathbf{R}$ . The Main Network’s hyper-parameters were fixed and we only tuned the hyper-parameters of Neurocoder, MOE and NSM. We report details of hyper-parameters in Table 5 and 6.

## Sequential learning experiments

**Synthetic polynomial auto-regression** A sequence was divided into  $n_{pa}$  chunks, each of which associated with a randomly generated polynomial. The degree and coefficients of each polynomial were sampled from  $U \sim [2, 10]$  and  $U \sim [-1, 1]$ , respectively. Each sequence started from  $x_1 = -5$  and ended with  $x_T = 5$ , equally divided into  $n_{pa}$  chunks. Each chunk contained several consecutive points  $(x_t, y_t)$  from the corresponding polynomial, representing a local transformation from the input to the output. Given previous points  $(x_{<t}, y_{<t})$  and the current  $x$ -coordinate  $x_t$ , the task was to predict the current  $y$ -coordinate  $y_t$ . To be specific, at each timestep, the Main Network GRU was fed with  $(x_t, y_{t-1})$  and trained to predict  $y_t$  by minimizing the mean square error  $1/T \sum_{t=1}^T (\hat{y}_t - y_t)^2$  where  $y_0 = 0$ ,  $\hat{y}_t$  is the prediction of the network and  $y_t$  the ground truth.

We augmented *GRU by applying Neurocoder* and HyperNet [12] *to the output layer of the GRU*. Here, the HyperNet baseline generated adaptive scales for the output weight of the GRU. We trained the networks with Adam optimiser with a batch size of 128. To balance the model size, we used GRU’s hidden size of 32, 28, 16 and 8 for the original Main Network, HyperNet, single-step and multi-step Neurocoder, respectively. We also excluded program integration phase in Neurocoders to keep the model size equivalent to or smaller than that of the Main Network. We report details of hyper-parameters for GRU, HyperNet and Neurocoder in Table 5 and 6.

We compared two configurations of Neurocoder - single-step, multi-head ( $J = 1, H = 15$ ) and multi-step, single-head ( $J = 5, H = 1$ )- against the original GRU with output layer made by MLP and HyperNet—a weight-adaptive neural network [12]. We found that MLP failed to learn and converge

within 10,000 learning iterations. In contrast, both Neurocoders learn and converge, in as little as only 2,000 iterations with the multi-step Neurocoder. HyperNet converged much slower than Neurocoders and could not minimize the predictive error as well as Neurocoders when Gaussian noise is added or the number of polynomials ( $n_{pa}$ ) is doubled (see Fig. 6).

**Atari 2600 games** We used OpenAI’s Gym environments to simulate Atari games. We used the standard environment settings, employing no-frame-skip versions of the games. The picture of the game snapshot was preprocessed by CNNs and the A3C agent was adopted from the original paper with default hyper-parameters as in [26]. *The actor/critic network of A3C was LSTM whose output layer’s working program was provided by Neurocoder or HyperNet.* The hidden size of the LSTM was 512 for all baselines. We list details of models and hyper-parameters in Table 5 and 6.

*Seaquest and MsPacman.* The original A3C agent was able to learn and obtain a moderate score of around 2,500 after 32 million environment steps. We also equipped A3C with HyperNet-based actors/critics, however, the performance remained unchanged, with scores of about 2/3 of Neurocoder-based agent’s.

## Continual learning experiments

**Split MNIST** We used the same 2-layer MLP and continual learning baselines as in [16]. Here, we again excluded program integration to avoid catastrophic forgetting happening on the residual program **R**. We only tuned the hyper-parameters of NSM and Neurocoder for this task. Remarkably, the NSM with much more parameters could not improve MLP’s performance, illustrating that simple conditional computation is not enough for continual learning (see Table 3).

**Split CIFAR** The 18-layer *ResNet* implementation was adopted from Pytorch’s official release whose weights was pretrained with ImageNet dataset. When performing continual learning with CIFAR images, we froze all except for the output layers of ResNet, which was a 3-layer MLP. We only tuned the hyper-parameters of SI and Neurocoder for this task. Details of model architectures and hyper-parameters are reported in Table 5 and 6.

In the CIFAR10 task, compared to the monolithic ResNet, the Neurocoder-augmented ResNet could achieve much higher accuracy when we finished the learning for all 5 tasks (55% versus 70%, respectively). Also, we realised that stressing the orthogonal loss further improved the performance. When we employed Synaptic Intelligence (SI [37]), the performance of ResNet improved, yet it still dropped gradually to just above 70%. In contrast, the Neurocoder-augmented ResNet with SI maintained a stable performance above 80% accuracy (see Fig. 8 (left)).

In the CIFAR100 task, Neurocoder alone with a bigger program memory slightly exceeded the performance of SI, which was about 10% better than ResNet. Moreover, Neurocoder plus SI outperformed using only SI by another 10% of accuracy as the number of seen tasks grew to 20 (see Fig. 8 (right)).

Notation	Meaning	Location	
		Program Controller	Program Memory
Trainable parameters			
$\theta^{u,v,\sigma}$	Composition network	✓	
$\phi$	Integration network	✓	
$\varphi^{u,v,\sigma}$	Key generator network		✓
$\mathbf{R}$	Residual program (optional)	✓	
$\mathbf{M}_U$	Memory of left singular vectors		✓
$\mathbf{M}_V$	Memory of right singular vectors		✓
$\mathbf{M}_S$	Memory of singular values		✓
Control variables			
$\xi_t^p$	Composition control signal	✓	
$\lambda_t^p$	Integration control signal	✓	
$k^{u,v,\sigma}$	Program keys		✓
$m^{u,v,\sigma}$	Program usages		✓
Hyper-parameters			
$P$	Number of memory slots		✓
$K$	Key dimension		✓
$l_I$	Number of considered least-used slots		✓
$J$	Number of recurrent attention steps	✓	
$H$	Number of attention heads	✓	
$a$	Orthogonal loss weight		✓

Table 1: Important parameters of Neurocoder.

Architecture	Task	Original	MOE	NSM	Neurocoder
MLP	CIFAR10	52.06	50.76	52.76	<b>54.86</b>
	CIFAR100	23.31	22.79	25.65	<b>26.24</b>
LeNet	CIFAR10	75.71	75.88	75.45	<b>78.92</b>
	CIFAR100	42.73	42.47	43.14	<b>47.21</b>
DenseNet	CIFAR10	93.61	80.61	94.24	<b>95.61</b>
	CIFAR100	68.37	38.20	64.53	<b>72.20</b>

Table 2: Best test accuracy over 5 runs on image classification tasks comparing original architecture, Mixture of Experts (MOE), Neural Stored-program Memory (NSM) and our architecture (Neurocoder). Three architectures of the Main Network of Neurocoder were considered: 3-layer perceptron (MLP), 5-layer CNN (LeNet [25]) and very deep Densely Connected Convolutional Networks (DenseNet [17]). We employed two classical image classification datasets: CIFAR10 and CIFAR100.

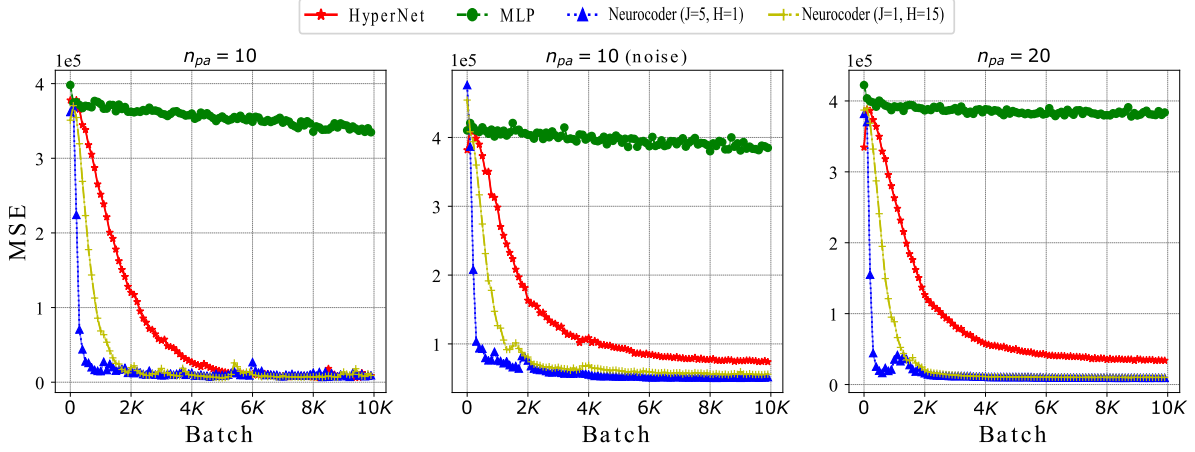


Figure 6: Polynomial auto-regression: mean square error (MSE) over training iterations with a batch size of 128 comparing HyperNet (red), MLP (green), multi-step (blue) and single-step (yellow) attention Neurocoders. All baselines use GRU as the Main Network. The learning curves are taken average over 5 runs.

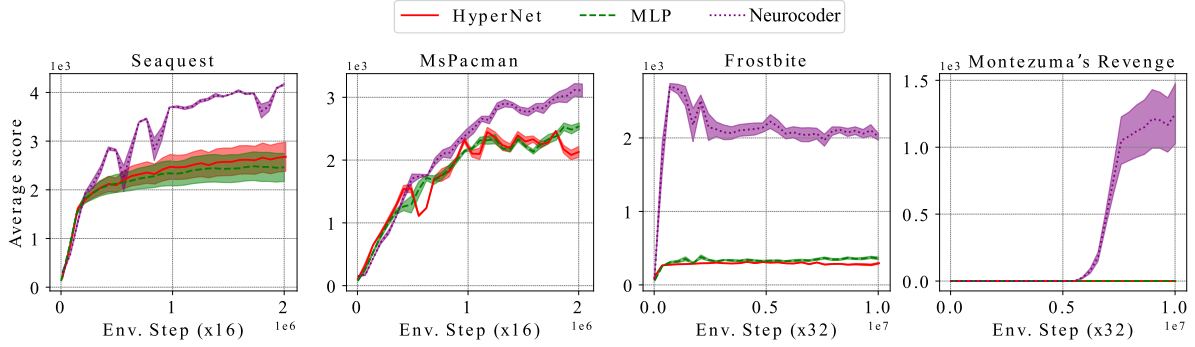


Figure 7: Learning curves (mean and std. over 5 runs) on representative Atari 2600 games. All baselines are applied to the actor/critic networks in the A3C agent.

Method	MLP [16]	MLP (ours)	NSM	Neurocoder
Adam	93.46 $\pm$ 2.01	93.75 $\pm$ 3.28	87.55 $\pm$ 4.38	<b>96.54<math>\pm</math>1.39</b>
Adagrad	98.06 $\pm$ 0.53	98.02 $\pm$ 0.89	96.63 $\pm$ 1.49	<b>99.01<math>\pm</math>0.19</b>
L2	98.18 $\pm$ 0.96	98.14 $\pm$ 0.43	91.44 $\pm$ 3.80	<b>98.35<math>\pm</math>0.74</b>
SI	98.56 $\pm$ 0.49	98.69 $\pm$ 0.20	98.87 $\pm$ 0.20	<b>99.14<math>\pm</math>0.24</b>
EWC	97.70 $\pm$ 0.81	97.00 $\pm$ 1.10	93.94 $\pm$ 2.36	<b>97.88<math>\pm</math>0.22</b>
O-EWC	98.04 $\pm$ 1.10	98.23 $\pm$ 1.17	96.11 $\pm$ 1.27	<b>98.30<math>\pm</math>1.48</b>

Table 3: Incremental task continual learning with Split MNIST. Final test accuracy (mean and std.) over 10 runs.

Method	MLP [16]	MLP (ours)	NSM	Neurocoder
Adam	55.16 $\pm$ 1.38	53.55 $\pm$ 1.27	54.85 $\pm$ 2.81	<b>58.46<math>\pm</math>0.46</b>
Adagrad	58.08 $\pm$ 1.06	57.83 $\pm$ 2.74	58.42 $\pm$ 1.87	<b>62.28<math>\pm</math>4.03</b>
L2	66.00 $\pm$ 3.73	64.37 $\pm$ 2.40	62.83 $\pm$ 7.21	<b>69.89<math>\pm</math>1.72</b>
SI	64.76 $\pm$ 3.09	64.41 $\pm$ 3.36	64.36 $\pm$ 2.99	<b>67.96<math>\pm</math>3.22</b>
EWC	58.85 $\pm$ 2.59	58.41 $\pm$ 2.37	58.12 $\pm$ 3.24	<b>65.66<math>\pm</math>1.25</b>
O-EWC	57.33 $\pm$ 1.44	57.78 $\pm$ 1.84	58.55 $\pm$ 3.40	<b>73.97<math>\pm</math>1.50</b>

Table 4: Incremental domain continual learning with Split MNIST. Final test accuracy (mean and std.) over 10 runs.

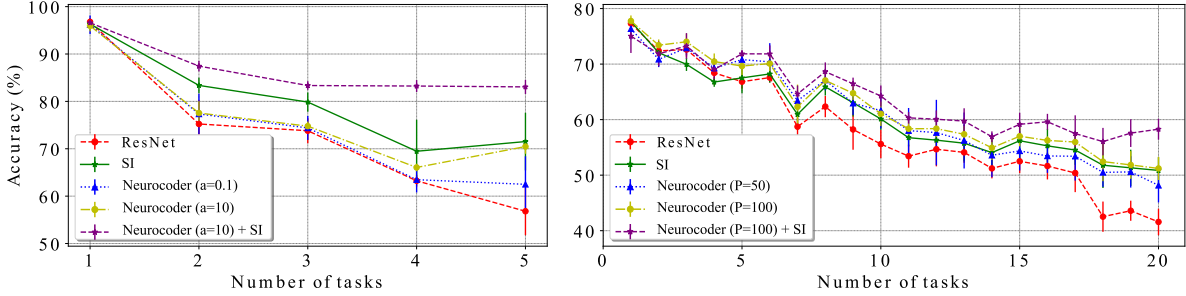


Figure 8: Incremental task continual learning with Split CIFAR10 (left) and CIFAR100 (right). Average classification accuracy with error bar over all learned tasks as a function of number of tasks.

Task	Neurocoder
MNIST	$P = 5, J = 5, H = 1$ $K = 2, l_I = 2, a = 0.1$
CIFARs	$P = 30, J = 5, H = 3$ $K = 5, l_I = 5, a = 0.1$
Polynomial	$P = 10, J = 1, H = 15$ $P = 20, J = 5, H = 1$
auto-regression	$K = 3, l_I = 2, a = 0.1$ $K = 3, l_I = 2, a = 0.1$
Atari games	$P = 80, J = 1, H = 15, K = 3, l_I = 5, a = 0.1$
Split MNIST	$P = 50, J = 1, H = 10, K = 5, l_I = 5, a = 10$
Split CIFARs	$P = 100, J = 1, H = 10, K = 5, l_I = 5, a = 10$

Table 5: Best hyper-parameters of Neurocoder in all experiments. – denotes not available. For polynomial auto-regression task, two Neurocoder configurations are tested, corresponding to single-step and multi-step Neurocoder. Across experiments, MOE and NSM employ 10 experts and 10 memory banks, respectively. HyperNet does not have any special hyper-parameters.

Task	Main Network	Original	MOE	NSM	HyperNet	Neurocoder	
MNIST	Linear classifier	7.8K	–	–	–	7.3K	
	3-layer MLP	1.7M	15.4M	21.2M	–	1.9M	
CIFARs	LeNet	2.1M	12.3M	27.1M	–	2.3M	
	DenseNet	7.0M	20.5M	16.7M	–	7.3M	
Polynomial auto-regression	GRU	3.4K	–	–	3.5K	3.6K	2.1K
Atari games	LSTM	3.2M	–	–	3.6M	3.3M	
Split MNIST	2-layer MLP	328K		2.3M		348K	
Split CIFARs	ResNet	12.6M	–	–	–	12.6M	

Table 6: Number of parameters of machine learning models in all experiments. The parameter count includes the parameter of the Main Network and the conditional computing model. – denotes not available. For tasks that contain different datasets, leading to slightly different model size, the numbers of parameters are averaged. For polynomial auto-regression task, two Neurocoder configurations are tested, corresponding to single-step and multi-step Neurocoder.